Seismic Behavior of Reinforced Concrete Piers Strengthened with Carbon Fiber Sheets

(Translated from Concrete Research and Technology, Vol. 8, No. 1, pp.189-203, Jan. 1997)

Koji OSADA

Shinya OHNO

Takahiro YAMAGUCHHI

Shoji IKEDA

Static and pseudo-dynamic tests using reinforced concrete column specimens were carried out to certify the effect carbon fiber sheets have on improving the ductility of reinforced concrete piers and to investigate the seismic properties of said piers after strengthening. From the experimental results, it was verified that the piers ductility can be improved by strengthening with carbon fiber sheets, and the optimum volume and area of carbon fiber sheets required for the strengthening were obtained. Also, it was shown that the rupture of carbon sheets in the horizontal direction occurred first at the corner of the column. The results of pseudo-dynamic tests confirmed that piers strengthened by carbon sheets could maintain well under an earthquake which had a maximum acceleration of 400gal.

Keywords: seismic strengthening, carbon fiber sheet, reinforced concrete pier, ductility, pseudo-dynamic test.

Koji OSADA is civil engineer at Japan Highway Public Corporation. He is a graduate of Tokushima University and obtained his Master's degree in 1991. He is a member of JSCE and JCI.

Shinya OHNO is a civil engineer in the 2nd Design Department, Civil Engineering Design Division of KAJIMA CORPORATION. He is a graduate of Yokohama National University and obtained his Master's degree in 1997. He is a member of JSCE and JCI.

Takahiro YAMAGUCHI is a research associate in Civil Engineering at Yokohama National University. He is a member of the JSCE, JCI, and JPCEA.

JSCE Fellow Shoji IKEDA is a professor of Civil Engineering at Yokohama National University. He served as the president of Japan Gas-Pressure Welding Association from 1989 to 1991 and as the president of the Japan Prestressed Concrete Engineering Association from 1993 to 1995. He is a member of IABSE, a fellow of ACI, and senior vice-president of FIP. He specializes in the design and mechanics of reinforced concrete, prestressed concrete and composite structures.

1. Introduction

In the Hanshin-Awaji Earthquake of 1995, reinforced concrete piers which had been designed and built in accordance with pre-1980 Specifications, in which the method of calculating shear and the design of terminated point use of longitudinal bars were revised, suffered especially severe damages. Because of this, piers are being reinforced as required to improve their load-bearing capacity and ductility.

Previously strengthen reinforced concrete piers, the RC jacket or steel jacket has been used. Recently, a new method of reinforcement using a carbon fiber sheet (CFS) which is thin and easy to handle is attracting attention. CFS was developed to apply carbon fibers to structures for reinforcement. The process of development and the characteristics of CFS are described concisely in literature [1]. In order to apply CFS to reinforced concrete structures, studies on the use of CFS to reinforce shear capacity, on terminated point of longitudinal bars, etc. have been carried out [1]-[4]. As a result, the applicability of CFS to those purposes has been confirmed. In fact, CFS has been employed to reinforce the shear capacity of the box girders of an RC bridge [5]. In order to employ the CFS jacket to effectively strengthen reinforced concrete piers, it is an essential prerequisite to clarify to what extent reinforcement with CFS improves ductility and seismic performance of existing piers.

The present experimental study was carried out to grasp the effect reinforcement with CFS has on the ductility and seismic performance of reinforced concrete piers. Scale models of actual piers (independent columns) were subjected to static and pseudo-dynamic load tests. In addition, using a dynamic video recorder [6] built in the pseudo-dynamic loading system, the dynamic response behavior and the process of fracture in the bridge pier were recorded on a video tape to study the seismic performance visually.

2. Experimental Procedure

2.1 Specimens

The reinforced concrete piers used as models in the present experiment (hereinafter referred to as existing piers) were independent two-column and wall type, of typical pier dimensions, designed and built in accordance with pre-1980 Specifications. The shapes of specimens are shown in Figure 1, and the specifications and experimental factors are shown in Table 1. While the dimensions of specimens are about 1/4 those of the existing piers, the tension bar and hoop ratios are equal. It should be noted, however, that since the hoops used are D6, the ratio of hoop spacing to column cross-sectional area is higher for the specimens than the existing piers. This might cause a slight difference between the existing piers and specimens in terms of the process of shear cracking and the time of longitudinal bar buckling. Even so, it is considered that the mode of failure remains unaffected. In order to achieve a clearer grasp of the effect reinforcement with CFS has on the ductility of piers, the specimen's longitudinal bars were not terminated in any way.

In this respect, the specimens differ from the existing piers which can be adversely influenced in sections without longitudinal bars.

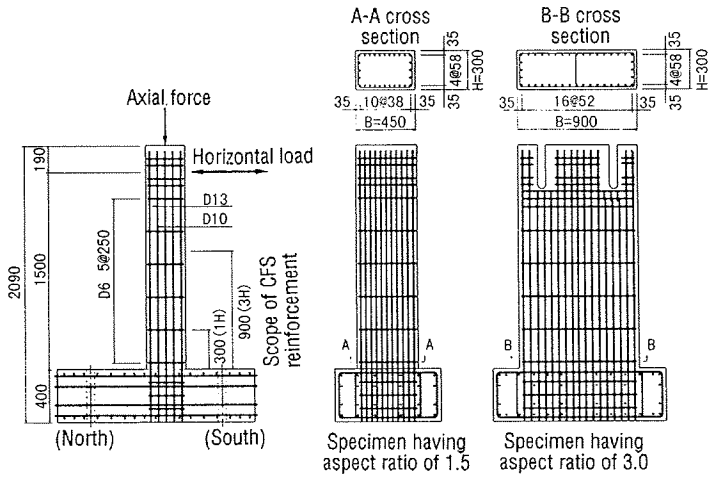

Fig. 1 Specimen shapes

Table 1 specimen characteristics and test factors

No.	Specimen name *1	sectional form B×H (mm)	Hoop reinforcement*2	CFS in hoop direction *3	longitudinal reinforcement *4	CFS in longitudinal direction
1	ST-N-1.5	450 × 300	D6@250 (0.056%)	- (0%)	22-D 13 6-D 10 (2.38%)	-
2	ST-CF-1.5			1 layer (0.05%)		1/4 layer
3	ST-2 CF-1.5			2 layers (0.1%)		
4	AST-CPB-1.5			2 layers (0.1%)		
5	AST 40-N-1.5			- (0%)		-
6	PD 45-N-1.5					
7	PD 20-CP-1.5			2 layers (0.1%)		1/4 layer
8	APD 40-CP-1.5					
9	PD 45-2 CF-1.5			2 layers (0.1%)		
10	AST-N-3.0	900 × 300	D6@250 (0.028%)	- (0%)	34-D 13 6-D 10 (1.76%)	-
11	AST-CP-3.0			4 layers (0.1%)		1/4 layer
12	PD 40-N-3.0			- (0%)		-
13	PD 40-CP-3.0			4 layers (0.1%)		1/4 layer

*1: ☆○-△-□

☆ [Specimen groups]
Specimen names beginning with "ST" or "PD": Group I
Specimen names beginning with "A": Group II
(Specimens of Group II were prepared after those of Group I were subjected to the load test, with consideration given to the results of the load test.)

○ [Loading method]
ST: Static load test
PD: Pseudo-dynamic load test
20: magnitude of maximum acceleration is 200gal equivalent
40: magnitude of maximum acceleration is 400gal equivalent
45: magnitude of maximum acceleration is 450gal equivalent

△ [Amount of CFS reinforcement in hoop direction]
N: without CFS lining
CF: CFS lining was executed in 1layer in the range up to 3*H* from the top end of footing, ρcf = 0.05%
2CF: CFS lining was executed in 2layers in the range up to 3*H* from the top end of footing, ρcf = 0.1%
CP: CFS lining was executed in 2layers or 4layers in the range up to 1*H* from the top end of footing, while in 1layer in the range from 1*H* to 3*H*,
ρcf = 0.1%; from 1*H* to 3*H*, ρcf = 0.05% for specimens with aspect ratio of 1.5,
ρcf = 0.1%; from 1*H* to 3*H*, ρcf = 0.03% for specimens with aspect ratio of 3.0
B: Area of CFS bonding in hoop direction = 1/4

□ [Cross-section shape (aspect ratio)]

*2: Parenthesized value is the ratio of hoop reinforcement.

*3: Parenthesized value is CFS area ratio (ρcf), which were obtained by the following equation.
$\rho cf = 2tcf/B \times 100(\%)$
where, *tcf*: design CFS thickness, B: cross-section width

*4: Parenthesized value is longitudinal bar ratios.

*5: For all specimens, the axial compressive load was 0.59 MPa.

Since the specimens were prepared in two different runs, there was a difference of about two months in the dates of concrete placement. In Table 1, the specimens whose names begin with A were prepared in the second run, and the other specimens were prepared in the first run. Hereafter, the specimens prepared in the first run shall be collectively called Group I and those prepared in the second run, Group II. Group II was prepared after considering the load-test results of Group I.

Specimens No. 1 through 9 each have a cross section whose height-to-width ratio (aspect ratio) is 1.5. Of these Nos. 1 through 4 were subjected to a static (ST) load test and Nos. 5 through 9 were subjected to a pseudo-dynamic (PD) load test to measure seismic performance. Specimens No. 10 through 13, modeled after a wall-type bridge pier, have an aspect ratio of 3.0. Nos. 10 and 11 were subjected to an ST load test and Nos. 12 and 13 were subjected to a PD load test. In Table 1, the specimens without CFS reinforcement correspond to the existing piers. The specimens reinforced with CFS differ in the amount of CFS and in the scope of reinforcement. For specimens No. 4, 7, 8, 11, and 13, the scope of CFS reinforcement in the hoop direction was determined after considering the results of the ST test on specimens No. 1 to 3. For each of those specimens, the section from the top end of the footing to 1*H* (*H*: height of cross section) is preponderately reinforced.

The arrangement of CFS fibers is unidirectional. The CFS reinforcement in the hoop direction was intended to improve the shear capacity and ductility of piers by the constraining effect on the concrete and longitudinal bars. In the longitudinal direction it was intended to prevent the CFS in the hoop direction from being damaged by flexural cracking and to ensure smooth stress transfer of the CFS in the hoop direction. Taking cost and workability into consideration, the amount of reinforcement in the hoop direction of existing piers is generally 0.05% to 0.1% in terms of area ratio. This is translated into one or two layers of CFS reinforcement for the specimens having an aspect ratio of 1.5 and two to four layers for the specimens having an aspect ratio of 3.0. In the present experiment, the number of CFS layers in the hoop direction for each specimen corresponds to the amount of reinforcement mentioned above.

Considering the bonding strength between CFS and the concrete of existing piers, one layer of CFS reinforcement in a specimen corresponds to four layers of CFS reinforcement in an actual bridge pier. In view of this, for specimen No. 4 (AST-CPB-1.5), the area of bonding between CFS and concrete was decreased by one-fourth. This was accomplished by marking off sheet of film into 20 mm × 20 mm squares and removing every one out of four squares. This sheet was inserted between the CFS in the hoop direction and the concrete.

In the present experiment, the longitudinal bars were not cut off. Therefore, assuming the existing bridge pier has one layer of CFS reinforcement, the reinforcement of the specimen with CFS in the longitudinal direction was made by bonding a 10 mm wide strip of CFS at intervals of 40 mm to secure the same area ratio as the existing bridge pier. The scope of reinforcement with CFS was from the top end of the footing to 3*H*. The second and subsequent layers of CFS in the hoop direction were up to 3*H* or 1*H* depending on specimens.

The procedure of bonding CFS to the concrete was accomplished in the following order : treatment of concrete, application of primer, bonding of CFS in the direction of longitudinal bars, impregnation of CFS with resin, bonding of CFS in the hoop direction, and impregnation of CFS with resin. Concerning the amount of lap in CFS layers, the results of a bonding test in which layers of CFS were bonded together showed that a lap length of at least 40 mm would be sufficient to secure the strength of CFS.[7] Although to be on the safe side, a lap length of 100 mm was used. The column corners were rounded to relieve the stress concentration on the CFS. According to the results of an experiment in which the relationship between CFS radius of curvature and tensile strength was obtained, the radius of curvature of CFS should be 10 mm or more. In view of this, the column corners were rounded to a radius of curvature of 30 mm.

2.2 Materials used

The CFS used for reinforcement was a carbon fiber sheet which was impregnated with epoxy resin after bonding to the concrete. CFS is made of carbon fibers which are evenly arranged unidirectionally on a thread woven into a reticular pattern. It is available in the form of a roll. The major characteristics of CFS are shown in Table 2. The epoxy resin used in bonding and impregnation of CFS is divided into three types--for spring/autumn (standard), for summer, and for winter--according to viscosity, hardening time, etc. The standard type was used for the specimens of Group I, and the winter type for Group II. The tensile strength of the resin itself is about 45 MPa after hardening.

Table 2 Mechanical properties of CFS

Design thickness (mm)	Fiber area weight (g/m^2)	Tensile strength *1 (MPa)	Young's modulus *1 (GPa)	Specimens *2
0.110	200	4 220	243	Group I
0.110	201	4 047	252	Group II

*1: The values of tensile strength and Young's modulus were obtained by a test using CFS specimens about 1 cm in width impregnated with standard resin (for spring/autumn).

*2: For Groups I and II, see Table 1.

Table 3 Mechanical properties of reinforcing bars

Size	Type	Yield strength	Tensile strength (MPa)	Young's modulus (GPa)	Specimens	application
D 6	SD 295	360	530	175	Group I	Hoop reinf.
D 10	SD 295	350	500	172		Longi. reinf. in web portion
D 13	SD 345	380	560	172		Longi. reinf.
D 6	SD 295	340	560	187	Group II	Hoop reinf.
D 10	SD 295	360	530	168		Longi. reinf. in web portion
D 13	SD 345	390	570	172		Longi. reinf.

reinf. :reinforcement

Longi. :longitudinal

Table 4 Mechanical properties of concrete

Compressive strength (MPa)	Tensile strength (MPa)	Young's modulus (GPa)	Poisson's ratio	Age (days)	Specimens
27	2.5	18	0.20	50	Group I (excludes PD 40-N-3.0)
31	2.2	18	0.20	42	PD 40-N-3.0
32	2.7	20	0.20	66	Group II

Mechanical properties of the reinforcing bars used in the specimens are shown in Table 3. Table 4 shows the mechanical properties of the concrete, obtained from the cylinder specimens, and cured under the same conditions as the specimens for loading tests.

Both the strength of D13 bar used for the longitudinal bars and the strength of concrete are somewhat higher for Group II than for Group I. The maximum size of aggregate used was 10 mm.

2.3 Loading method

In the ST and PD load tests, two actuators were used to apply a lateral load to each specimen while applying a specified axial force to the top of the specimen, as shown in Figure 1. The footing of each specimen was fixed to the reaction bed with PC bars. Taking the weight of the superstructure into account, an axial compressive force of 0.59 MPa was used for all the specimens. The test loads were applied in the direction of bridge axis (the south-north direction in Figure 1). In the sections that follow, the push loads and displacements toward north are prefixed with a positive sign (+) and those toward south are prefixed with a negative sign (-).

The ST load test procedure is as follows.
A positive load and a negative load are applied once at each stage of displacement until the end of loading while increasing the displacement by 1 δy. 1 δy is the average value of positive and negative displacements obtained during application of the calculated lateral load at which the tensile stress in the outside longitudinal bars reaches its yield value. Positive and negative loads were applied only once for each stage of displacement because the results of various past PD load tests found the number of times a large deformation occurs in a structure during a big earthquake to be not more than one. The specimens without CFS reinforcement were subjected to the ST load test first, regardless of their aspect ratio (1.5 or 3.0), and the yield displacement (δy) obtained with these specimens was also used for the specimens reinforced with CFS.

δy was obtained as follows. In order to calculate the static inelastic displacement easily and accurately, a one-dimensional model considering the rotation at the bottom of a column was proposed. To evaluate the rotation at the bottom of a column, the joint portion of the column and the footing is assumed to be H/2 below the surface of the footing. Furthermore, since the column and the footing are replaced as one dimensional members in the model, the reaction point is assumed to be H/4 above the surface of the footing in accordance with the two dimensional effect.

The initial setting values used in the PD load test are shown in Table 5. The seismic wave used is 15 seconds of the NS component observed at the Kobe marine meteorological observatory during the Hanshin-Awaji Earthquake. The input wave was obtained by eliminating the preliminary tremor to make the time of maximum acceleration occurrence 2.55 seconds. The solution of the vibration equation in the PD load test was obtained using the central difference method. From the accuracy of the solution, the time interval was determined to be 0.01 seconds. Therefore, in the experiment, load was applied in 1,500 steps in 15 seconds. From the bridge pier under consideration, the natural period was assumed to be 0.3 seconds. For the stiffness that is required to determine the virtual lumped mass, the initial stiffness before the occurrence of a crack was used. The virtual lumped mass was calculated from the natural period and initial stiffness assuming the member as a single-degree-of-freedom system. From the results of a past study [9], the damping ratio (h) was assumed to be 0.03 before yielding of the longitudinal bars and 0 after that.

Table 5 Data used in pseudo-dynamic tests

Specimen	Natural period (s)	stiff-ness (MN/m)	Virtual lumped mass (t)	Damping ratio *1	Yield displace-ment*2 (mm)	Acceleration level *3	Maximum acceleration *3 (cm/s²)
APD 40-N-1.5	0.3	18.6	42	0.03	13.9	①400 gal equivalent	298
						②400 gal equivalent	298
PD 45-N-1.5						①200 gal equivalent	146
						②450 gal equivalent	335
PD 20-CP-1.5						①200 gal equivalent	146
APD 40-CP-1.5						①400 gal equivalent	298
						②400 gal equivalent	298
PD 45-2CF-1.5						①200 gal equivalent	146
						②450 gal equivalent	335
PD 40-N-3.0		24.5	56		12	①200 gal equivalent	170
						②400 gal equivalent	346
PD 40-CP-3.0						①200 gal equivalent	170
						②400 gal equivalent	346

*1: Damping ratio (h) is assumed to be 0 after the longitudinal reinforcement yields.

*2: The yield displacement for specimens having an aspect ratio of 1.5 was obtained by an ST load test on specimen ST-N-1.5, and the yield displacement for specimens having an aspect ratio of 3.0 was obtained by calculation using the fiber model.

*3: ①indicates the first loading and②, the second loading.

The maximum accelerations of input waves are as shown in Table 5. The numbers ① and ② indicate the first loading and the second loading, respectively. The second loading was applied to the same specimen after completion of the first loading. The meaning of "acceleration equivalent to 0.2 g" in Table 5 is this: The acceleration obtained from the load and lumped mass at the time when the longitudinal bars stress, calculated by the fiber model, becomes 294 MPa, which is divided by 1.25

the correction value for the appropriate natural period taking the response into account, provided in the Road Bridge Specifications. [10] The value obtained in this way is assumed as the ground acceleration equivalent to 0.2 g in the design of an actual bridge. By this, the acceleration is made to correspond to that of an actual structure. The acceleration equivalent to 400 gal (450 gal) was obtained by a proportional calculation using the acceleration equivalent to 0.2 g.

2.4 Measuring method

Displacement relative to the column footing was measured at three different points 1,500 mm (the same height at which the horizontal load was applied), 750 mm, and 50 mm from the top end of the footing. The values of displacement shown below are those measured at the loading point. Strain was measured by strain gages attached to suitable points of the longitudinal bars and hoops. Strain gages were also attached to the surfaces of the concrete and CFS to measure the constraining effect of CFS. Cracks were measured on the west side (see Figure 1).

Video recording in the PD load test was effected every 0.03 seconds during the occurrence of seismic waves. The recording time of one still picture was 1 frame per 1/30 second. In this case, the total recording time of seismic data is about 16.7 seconds, and the pictures reproduced at the standard speed nearly correspond to the actual time scale. Two video cameras were used, one for recording the behavior of the entire specimen and one for recording only the area ranging from the bottom of the column to 1.5H.

3. Results of ST Load Test and Consideration

3.1 Load-bearing behavior and ductility

The results of the ST load test are shown in Table 6. The yield displacement (δy) of specimen ST-N-1.5 (without CFS reinforcement) was 13.9 mm and the yield displacement ($\delta y'$) of specimen AST-N-3.0 was 12.2 mm. Because of the limited stroke of the actuators, the maximum displacement of each specimen under load was seven to eight times the yield displacement.

The envelopes of the lateral load-displacement curves obtained by the load tests on specimens ST-N-1.5, ST-CF-1.5, and ST-2CF-1.5 and the values calculated using the fiber model are shown in Figure 2. The calculated values are those obtained up to the concrete compressive strain reaching 5,000 μ assuming that a gradually-increasing unidirectional load was applied to ST-N-1.5. The calculated values agree with the experimental values so well that they cannot be discriminated from each other. The values on the vertical axis are divided by calculated yield load ($P y$) of ST-N-1.5, and the values on the horizontal axis are divided by measured yield displacement (δy) of ST-N-1.5.

Table 6 Results of ST load test

Specimen	Final load applied	Maximum lateral load*1	Residual lateral load*2	Toughness ratio	Remarks
ST-N-1.5	±7 δy	+110 kN -111 kN	+33 kN (30%) -16 kN (14%)	3	· Longitudinal bars buckled and covering concrete exfoliated during application of -4 δy · Cracks occurred over wide range
ST-CF-1.5	±7 δy	+115 kN -118 kN	+86 kN (75%) -82 kN (70%)	5	· CFS in range from bottom of column to 1H began to bulge during application of -5 δy . · CFS fractured during application of -6 δy
ST-2 CF-1.5	±7 δy (five times)	+116 kN -118 kN	+106 kN (92%) -109 kN (93%)	7 or more	· CFS in range from bottom of column to 1H began to bulge during application of -5 δy . · CFS lap separated during application of -7 δy (first time). · CFS in direction of main reinforcement fractured during application of -7 δy (fifth time).
AST-CPB-1.5	±6.9 δy (five times) (application +8 δy stopped halfway)	+120 kN -121 kN	+112 kN (93%) -112 kN (93%)	7 or more	· CFS in range from bottom of column to 1H began to bulge during application of -5 δy . · CFS fractured during application of -6.9 δy (first time).
AST-N-3.0	±7 δy	+179 kN -176 kN	+92 kN (51%) -108 kN (61%)	4	· Longitudinal bars buckled and covering concrete exfoliated during application of -5 δy .
AST-CP-3.0	±7.8 δy	+185 kN -183 kN	+157 kN (85%) -158 kN (86%)	7 or more	· CFS in range from bottom of column to 1H began to bulge during application of -5 δy . · CFS did not fracture.

*1: top number indicates the maximum lateral load on the positive side and bottom number, on the negative side.

*2: Residual lateral load at the displacement at which the application of load is terminated. Figures in parentheses indicate ratios to maximum lateral load.

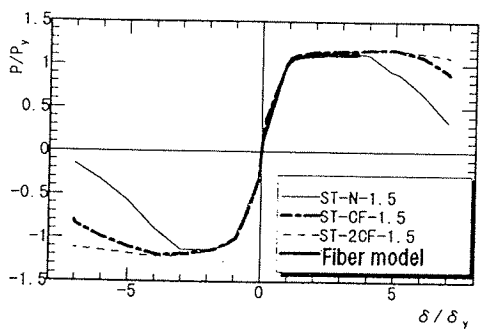

Fig. 2 Envelopes of lateral load-displacement curves

In specimen ST-N-1.5, diagonal cracks developed markedly at around 4 δy, causing the longitudinal bars to buckle, the covering concrete to exfoliate, and the lateral load to decline. Under a load of -7 δy, the residual lateral load became 16 kN, suggesting that the specimen almost lost its resistance against lateral load . The range of fracture was wide and a large vertical crack running along the longitudinal bars from the top end of the footing to a height of about 3H was observed. In the range up to 1H, even the concrete inside the hoops fractured. In specimen ST-CF-1.5 which was reinforced with one layer of CFS in the hoop direction, the CFS on the compression side began to bulge in the range from the top end of the footing to 1H while a load of -5 δy was being applied, causing the lateral load to decline. It is thought that the longitudinal bars buckled at this point of time. Under a load of -6 δy, the CFS in the hoop direction, which had begun bulging, fractured with a loud noise near the corner of the column. The CFS in the longitudinal direction also fractured at the same time. Specimen ST-2CF-1.5 reinforced with two layers of CFS did not show a marked decline in lateral load even when it was subjected to a load of -7 δy. Therefore, the load test on this specimen was finished after 7 δy and -7 δy were alternately applied to it five times. The residual lateral load after the first loading was 93% of the maximum lateral load . Even after the fifth loading, the specimen still retained 70% of its maximum lateral load . As in specimen ST-CF-1.5, the damage concentrated in the area from the top end of the footing to a height of 1H. When a load of -5 δy was applied, the CFS began to bulge slightly. When a load of -7 δy was applied for the first time, the lap between the two carbon fiber sheets separated. At the fifth application of 7 δy, the CFS in the longitudinal direction fractured and the damage to the CFS at the lap became more conspicuous. It seemed that the lap should have been a little longer. It was confirmed that when the aspect ratio is 1.5, the longitudinal bars of a specimen reinforced with CFS buckle at a displacement about 1 δy larger than that of a specimen without reinforcement; and that by securing an area ratio of 0.1% for the CFS, the lateral load does not decline markedly even under a load of 7 δy. Concerning the range of reinforcement, it was found that the area from the top end of the footing to 1H is important. Photo 1 shows the conditions of specimens under a load of -7 δy. The degree of damage to the specimen without CFS reinforcement differs noticeably from that of the specimens reinforced with CFS. Thus, the effect of CFS reinforcement in maintaining the soundness of piers is evident.

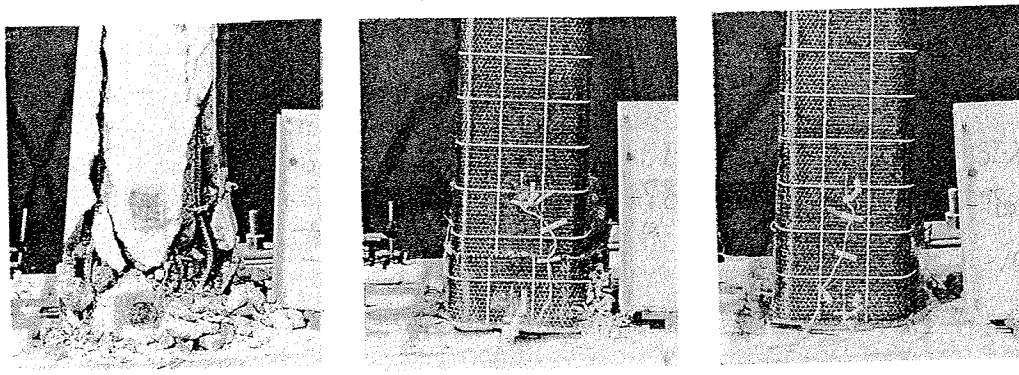

ST-N-1.5 ST-CF-1.5 ST-2CF-1.5

Photo 1 Conditions of specimens under -7 δy

(specimens having aspect ratio of 1.5)

The envelopes of lateral load-displacement curves obtained with specimens having an aspect ratio of 3.0 are shown in Figure 3. When the aspect ratio is 3.0, the calculated yield load is about 10% smaller than the yield load on the envelope of the positive side and nearly equal to the experimental value on the negative side. The tensile strain in the longitudinal bars at the bottom of the column under the calculated yield load almost reached the yield strain--1,900 to 2,000--on the positive and negative sides.

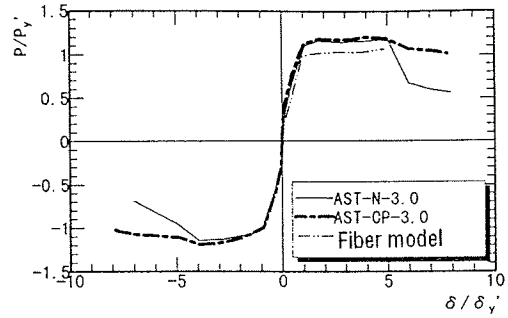

Fig. 3 Envelopes of lateral load-displacement curves

In specimen AST-N-3.0 without CFS reinforcement, diagonal cracks showed marked development under a load of 4 $\delta y'$. When a load of -5 $\delta y'$ was applied, all the longitudinal bars on the compression side buckled and concrete across the column width exfoliated in the area up to 1.5H, causing the lateral load of the specimen to decline to 84% of its maximum lateral load. Under a load of 7 $\delta y'$, the residual lateral load was 50% of the maximum value. In the case of specimen AST-CP-3.0, unlike the case of specimens having an aspect ratio of 1.5, the CFS reinforcement did not markedly shift the buckling point of the longitudinal bars. As in the specimen without CFS reinforcement, the longitudinal bars of AST-CP-3.0 buckled and the CFS bulged with a loud noise under a load of -5 $\delta y'$. However, the decline in lateral load was small: the specimen retained 95% of its maximum lateral load . The amount of CFS reinforcement was increased only in the area from the top end of the footing to 1H to secure an area ratio of 0.1%. Nevertheless, even under a load of 7 $\delta y'$, the CFS did not fracture and the lateral load remained as large as 87% of the maximum value.

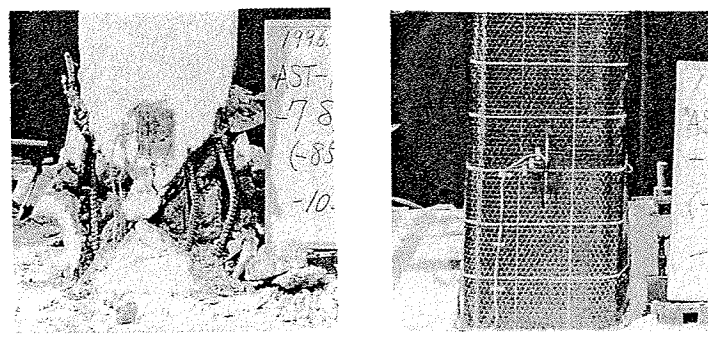

AST-N-3.0 AST-CP-3.0

Photo 2 Conditions of specimens under -7 δy (specimens having aspect ratio of 3.0)

Photo 2 shows the conditions of specimens under a load of -7 $\delta y'$. As in the case of specimens having an aspect ratio of 1.5, the degree of damage to the specimen without CFS reinforcement differs markedly from that of the specimen reinforced with CFS.

Assuming the ultimate displacement of each specimen as its maximum displacement that is not below the calculated yield load (Py) on the load-displacement curve and assuming the maximum displacement divided by δy, when the aspect ratio is 1.5, or by $\delta y'$, when the aspect ratio is 3.0, as the ductility ratio of the specimen, the ductility ratio was 3 for ST-N-1.5 without CFS, 4 for AST-N-3.0 without CFS, 5 for ST-CF-1.5 with 0.05% CFS reinforcement, and 7 or more for ST-2CF-1.5 and AST-CP-3.0 both with 0.1% CFS reinforcement. The difference in resistance against lateral load between specimens with and without CFS reinforcement was 7% at most, and the improvement of flexural lateral load by CFS in the longitudinal direction was small.

3.2 Characteristics of crack occurrence and damage at the bottom of the columns.

Figure 4 shows the cracking characteristics of specimens ST-N-1.5, ST-CF-1.5, and ST-2CF-1.5 under a load of -4 δy. Under -4 δy, the specimens reinforced with CFS were free from CFS bulging due to the buckling of longitudinal bars and showed only minor cracks at column bottoms and around $3H$ where there was no CFS reinforcement. Apparently, the CFS of these specimens remained unaffected. In the case of specimen ST-CF-1.5, the maximum crack width was 4.0 mm at the bottom of the column and 0.04 mm or less at, and around $3H$, indicating clearly that cracks concentrated at the column bottoms. In specimen ST-N-1.5 without CFS reinforcement, the longitudinal bars on the compression side buckled and the concrete exfoliated markedly under -4 δy. In addition, several cracks, which are considered due to a bonding fracture, occurred along the longitudinal bars on the tension side. Those cracks occurred in the entire column. Photo 3 shows the conditions at the column bottoms of three specimens after the exfoliated concrete was removed (for the specimens reinforced with CFS, the CFS from the center of the north side to the center of the south side of the column was also removed) at the end of the load test. From this photo, it can clearly be seen that while the longitudinal bars of ST-N-1.5 without CFS reinforcement buckled, the specimens with CFS reinforcement were free from shear fracture and had only local damage. In particular, ST-2CF-1.5 reinforced with CFS at an area ratio of 0.1% is completely free from shear damage.

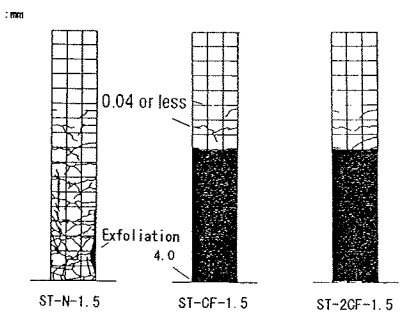

Fig. 4 Cracking characteristics (under -4 δy)

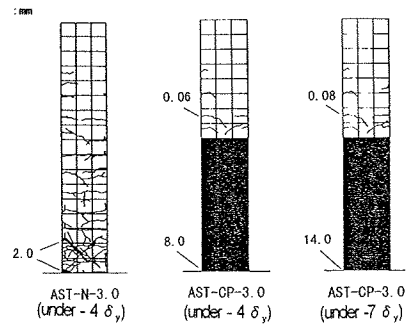

Fig. 5 Cracking characteristics

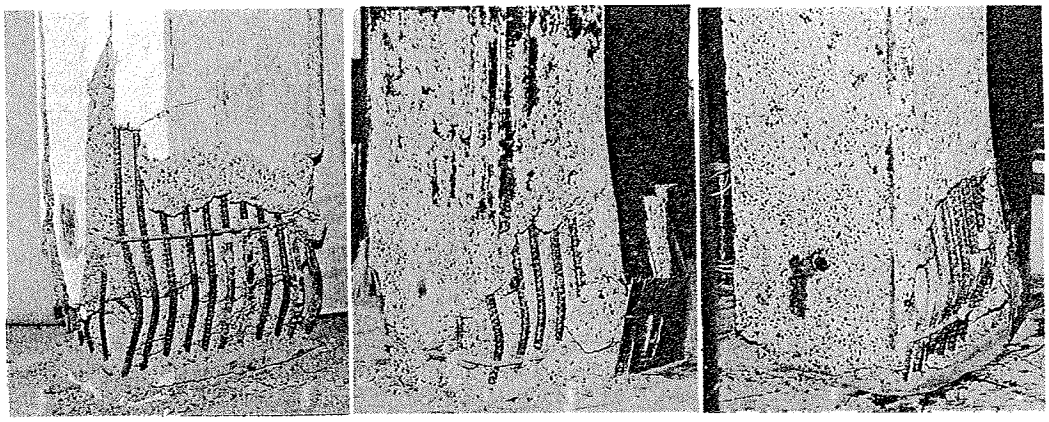

ST-N-1.5 ST-CF-1.5 ST-2CF-1.5

Photo 3 Conditions at the bottom of columns at end of load tests (aspect ratio :1.5)

Figure 5 shows the cracking characteristics of specimen AST-N-3.0 under $-4\ \delta y'$ and specimen AST-CP-3.0 under $-4\ \delta y'$ and $-7\ \delta y'$. Under $-4\ \delta y'$, both specimens were free from longitudinal bar buckling. In the case of AST-N-3.0 without CFS reinforcement, wide and marked cracks concentrated at the bottom of the column. In addition, large, diagonal cracks can be observed. The maximum width of cracks was 2.0 mm for both a bending crack at the bottom of a column and diagonal crack. The crack width under $-7\ \delta y'$ could not be measured because the concrete collapsed. The cracking characteristics in AST-CP-3.0 reinforced with CFS under $-4\ \delta y'$ was similar to that in specimen AST-CPB-1.5 having an aspect ratio of 1.5.

Namely, no change was observed in the CFS and cracks occurred only at the bottom of columns and around $3H$ where there was no CFS reinforcement. The maximum crack width was 8.0 mm for cracks at the bottom of columns and 0.06 mm for cracks in the section around $3H$. Under $-7\ \delta y$, the longitudinal bars buckled and the maximum crack width increased to 14.0 mm and 0.08 mm, respectively. Photo 4 shows the conditions at the bottom of the columns of AST-N-3.0 and AST-CP-3.0 at the end of the load test. The buckling of the longitudinal bars of AST-N-3.0 and the bulging of CFS of AST-CP-3.0 can be clearly seen.

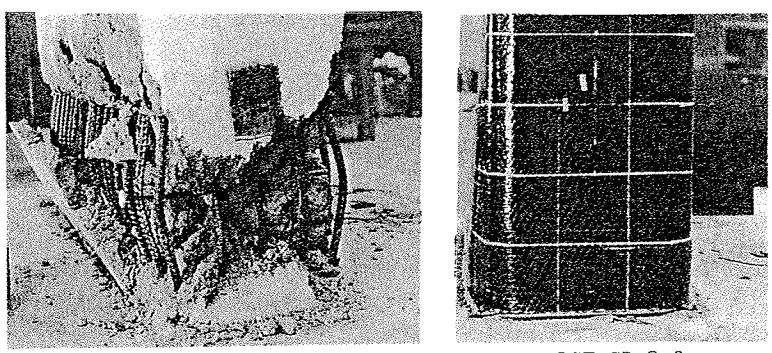

AST-N-3.0 AST-CP-3.0

Photo 4 Conditions at the bottom of columns at end of load tests (aspect ratio : 3.0)

3.3 Effect of bonding between CFS and concrete

Figure 6 compares the envelopes of load-displacement curves obtained through the load tests on specimens ST-2CF-1.5 and AST-CPB-1.5 in which the area of bonding between the CFS in the hoop direction and concrete was reduced to 1/4. Since the longitudinal bars used in the two specimens somewhat differ in yield load , there is a difference of 3% in maximum lateral load . However, the two envelopes look almost the same in shape. This suggests that the difference in bond strength between the CFS and concrete has minimal effect on the load-carrying behavior of the members. Therefore, the improvement of ductility by CFS reinforcement, as verified with specimens, can reasonably be expected in an actual structure too. A marked difference in behavior between the two specimens was the damage characteristics of CFS caused by a large deformation. In ST-2CF-1.5, the two layers of CFS ultimately separated at the lap. In AST-CPB-1.5, by contrast, the CFS in the hoop direction fractured at several points. Whether this difference was due to a difference in bond properties or due simply to experimental error could not be judged from the results of the present test alone. Photo 5 shows the condition of the compression side of AST-CPB-1.5 during the fifth application of $-6.9\,\delta y$. It can be seen that the CFS in the hoop direction fractured into separate strips at a corner of the column.

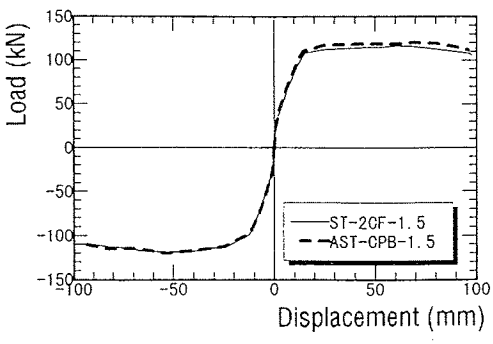

Fig. 6 Envelopes of lateral load-displacement curves

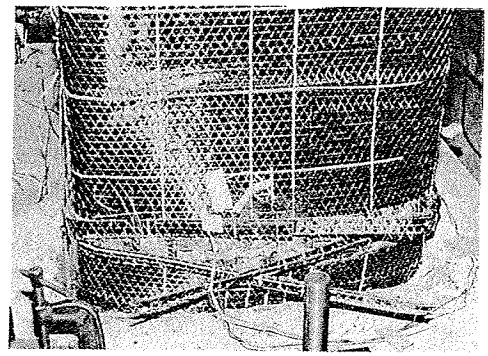

AST-CPB-1.5

Photo 5 Condition of south side during the fifth application of $-6.9\,\delta y$

4. Results of PD Load Test and Some Observations

4.1 Response behavior during an earthquake

(1) Acceleration equivalent to 0.2 g

The load-response displacement curve obtained when a seismic wave equivalent to 0.2 g--the design earthquake acceleration--was applied to PD 45-N-1.5 without CFS reinforcement, which corresponds to the existing bridge pier, and the condition of cracking 15 seconds after the PD load test are shown in Figure 7.(a) and (b). The maximum response displacement was 23 mm, about 1.7 times of δy. Though bending cracks were observed, neither diagonal cracks nor collapse of the concrete occurred and the specimen was free from a decline in lateral load . The maximum residual crack width 15 seconds after the load test was 0.3 mm

at the columns bottom. From these results, it could be confirmed that the existing piers had sufficient seismic performance against the earthquake assumed in the design. PD 45-2CF-1.5 with CFS reinforcement also showed a sound response behavior at an acceleration equivalent to 0.2 g. It did not show any decline in lateral load and was almost free of damage. The maximum response displacement was about 1.4 δy, which was smaller than that of PD 45-N-1.5.

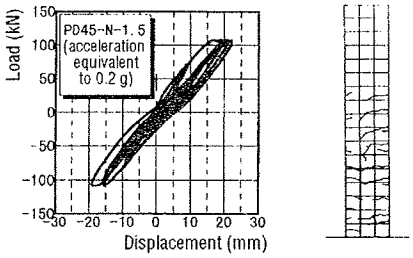

(a)Load-response displacement (b)Condition of cracking (at 15 seconds)

Fig. 7 PD 45-N-1.5 (acceleration equivalent to 0.2 g)

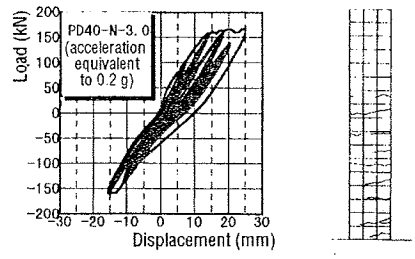

(a)Load-response displacement (b)Condition of cracking (at 15 seconds)

Fig. 8 PD 40-N-3.0 (acceleration equivalent to 0.2 g)

The load-response displacement curve obtained from the results of the load test on PD 40-N-3.0 (aspect ratio: 3.0) and the cracking characteristics 15 seconds after the load test are shown in Figure 8(a) and (b). The maximum response displacement was 25 mm, about two times of $\delta y'$. Like the specimens having an aspect ratio of 1.5, PD 40-N-3.0 showed a sound load-carrying behavior free from major damage and decline in lateral load at an acceleration equivalent to 0.2 g--the earthquake assumed in the design. PD 40-CP-3.0 with CFS reinforcement also showed a sound behavior. The maximum response displacement was 17 mm, or about 1.4 δy, which was smaller than that of PD 40-N-3.0.

Figure 9 compares response displacement between PD 45-2CF-1.5 and PD 20-CP-1.5. For experimental reasons, the PD load test on PD 20-CP-1.5 was terminated 7.94 seconds after the occurrence of a seismic wave. The comparison was made to measure the differences of effects in reinforcement of the second layer of CFS in the hoop direction between two ranges--from the top end of the footing to $3H$ and to $1H$. However, the two specimens showed no marked difference in response displacement behavior.

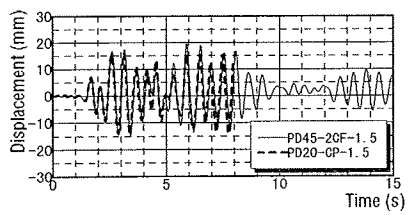

Fig. 9 Comparison of displacement response curves (acceleration equivalent to 0.2 g)

(2) Acceleration equivalent to 400 gal

A PD load test was carried out assuming the maximum acceleration of the

acting seismic wave as being equivalent to 400 gal--about two times the acceleration of the earthquake assumed in the design. Figure 10(a) and (b) show the load-response displacement curves obtained with APD 40-N-1.5 (without CFS) and APD 40-CP-1.5 (with CFS) during the first loading test. Figure 11 compares response displacement between the two specimens. Both specimens showed nearly the same maximum response displacement--about 5 δy--and a response behavior drift to the positive side. In APD 40-N-1.5 (without CFS), the longitudinal bars on the negative side buckled, causing a decline in lateral load . After that, the response period became somewhat longer. Looking at the video images of APD 40-CP-1.5, the CFS at the columns bottom was bulging and restoring. At the end of the test, however, neither a change of CFS appearance due to exfoliation of concrete nor a decline in lateral load was observed.

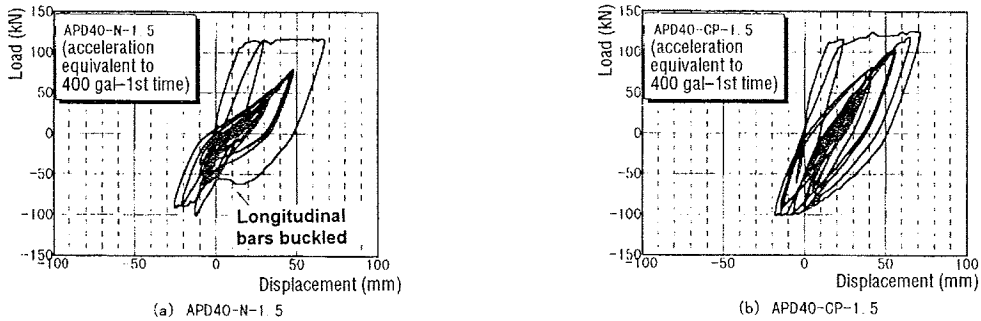

Fig. 10 Lateral load - displacement response curves (acceleration equivalent to 400 gal--1st time)

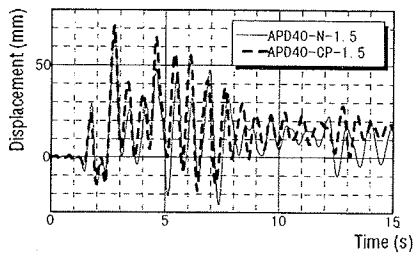

Fig. 11 Comparison of displacement response curves (acceleration equivalent to 400 gal--1st time)

Taking the drift of response displacement into consideration, the response properties were observed in terms of the sum of maximum positive and negative response displacements (hereinafter called the total amplitude). The total amplitude was 93 mm for APD 40-N-1.5 and 90 mm for APD 40-CP-1.5. Under seismic forces equivalent to 400 gal, the presence or absence of CFS reinforcement made a marked difference in lateral load and damage to appearance. Even so, there was not much difference in response displacement between the two specimens.

Figure 12 compares load-response displacement curves between the two specimens when a seismic force equivalent to 400 gal acted on them a second time. During the test, the response displacement exceeded the capacity of the actuator stroke. Therefore, the application of load to APD 40-N-1.5 was terminated 2.82 seconds after the time of occurrence

of the seismic wave passed. Similarly, the application of load to APD 40-CP-1.5 was terminated 2.55 seconds after the time of occurrence of 2.71-sec maximum acceleration passed. In APD 40-N-1.5, the longitudinal bars on both the positive and negative sides (south and north sides) buckled and the lateral load declined to about one-half of the maximum value, showing an inverted S-shaped hysteresis behavior. In APD 40-CP-1.5, by contrast, only the longitudinal bars on the negative side (south side) buckled and the lateral load remained unchanged, maintaining a spindle-shaped hysteresis behavior. It can clearly be seen from this that CFS reinforcement is also effective in securing the safety of structures during the period of after-tremor. Photo 6 shows the conditions of the two specimens after application of the final load. As the results of the ST load test indicated, the degree of damage depends largely on the presence or absence of CFS reinforcement.

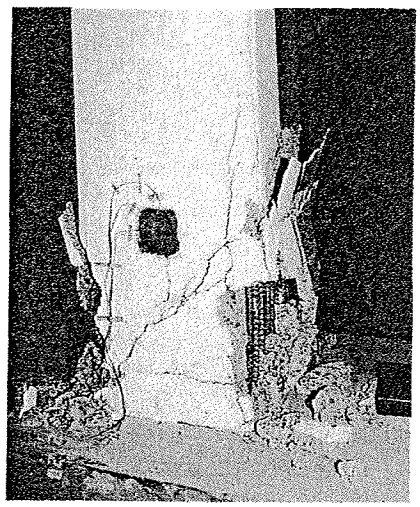

APD 40-N-1.5 (at 2.82 sec)

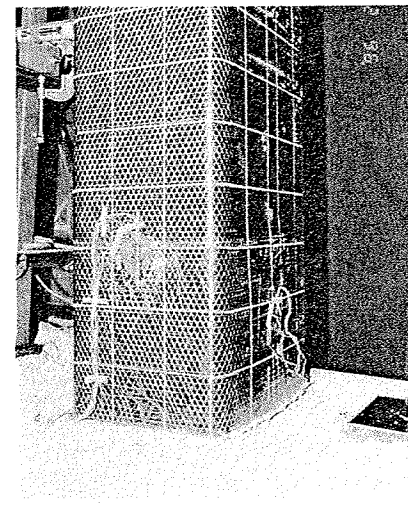

APD 40-CP-1.5 (at 2.71 sec)

Photo 6 Conditions of specimens subjected to second application of acceleration equivalent to 400 gal

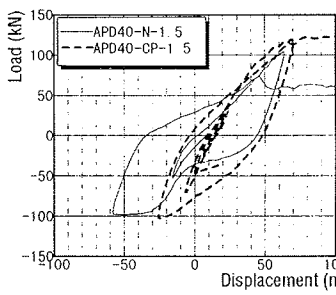

Fig. 12 Comparison of Lateral load - displacement response curves (acceleration equivalent to 400 gal)

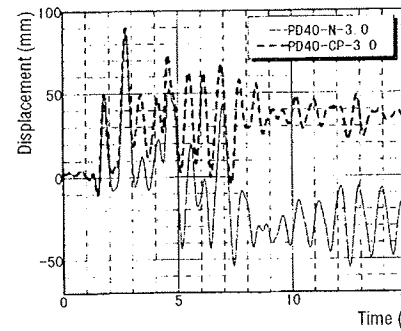

Fig. 13 Comparison of displacement response curves (acceleration equivalent to 400 gal)

Figure 13 compares response displacement curves obtained when seismic

wave equivalent to 400 gal was input to specimens having an aspect ratio of 3.0. It should be noted that these specimens are the same ones that had been subjected to a test using a seismic wave equivalent to 0.2 g. PD 40-N-3.0 (without CFS) suffered diagonal cracks at the bottom of column, 2.73 seconds after the occurrence of the seismic wave, and recorded a maximum response displacement of 7 $\delta y'$ on the positive side 0.01 seconds later. After the specimen experienced the maximum response displacement, the longitudinal bars buckled and the concrete showed marked exfoliation at 3.09 seconds when the deformation returned to 0 for the first time. Thereafter, as the concrete continued to deteriorate, the response drifted toward the negative side. At 12.52 seconds, a maximum displacement of 4.8 $\delta y'$ was recorded on the negative side and the lateral load declined to about 70% of the maximum value. In PD 40-CP-3.0 (with CFS), the displacement became maximum on the positive side at 2.73 seconds, the maximum displacement being 7.3 $\delta y'$ comparable to that of PD 40-N-3.0. Though horizontal cracks were observed in the resin-bonded portion of CFS, the CFS did not fracture until the end of the experiment. After the specimen experienced the maximum response displacement, the CFS from the top end of the footing to 1H began to bulge at 3.06 seconds when the deformation returned to 0 for the first time. Thereafter, the response shifted toward the positive side, but the lateral load remained unaffected. The total amplitude was 140 mm for PD 40-N-3.0 and 100 mm for PD 40-CP-3.0. Unlike the case of specimens having an aspect ratio of 1.5, reinforcement with CFS reduced the total amplitude to 70%. This is not ascribable to the difference in aspect ratio. The real reason is probably that the present application of a load equivalent to 400 gal was the second time (a load was applied to the same specimen the first time PD 40-N-3.0 and PD 40-CP-3.0 experienced a load equivalent to 200 gal), hence the degree of damage and the amount of displacement of the specimens became larger, thereby making the effect of CFS reinforcement greater.

(3) Acceleration equivalent to 450 gal

Figure 14 compares the load-response displacement curves obtained by applying a seismic wave equivalent to 450 gal to the specimens which had been previously subjected to a test using a seismic wave equivalent to 0.2 g. As in the experiment using the seismic wave equivalent to 400 gal, both specimens showed a response displacement exceeding the actuator capacity. Therefore, the experiment was terminated when a deformation of about 7 δy occurred at 2.69 seconds for PD 45-N-1.5 and at 2.70 seconds for PD 45-2CF-1.5. Unlike the results of the ST load test, both specimens showed marked deformation in one direction, hence the lateral load remained the same until a deformation of 7 δy occurred. At 2.67 seconds, immediately before the application of load was terminated, PD 45-N-1.5 showed marked development of diagonal cracks at the bottom of the column. In PD 45-2CF-1.5, as in the case of PD 40-CP-3.0 (aspect ratio: 3.0 and subjected to an acceleration equivalent to 400 gal), horizontal cracks occurred in the CFS resin on the tension side at the bottom of the column, however, rupture of CFS was not observed. Thereafter, when the displacement of each specimen was returned to 0, the longitudinal bars of PD 45-N-1.5 buckled at the bottom of the column and the covering concrete exfoliated. In PD 45-2CF-1.5, the CFS began to bulge in the area from the top end of the footing to 1H.

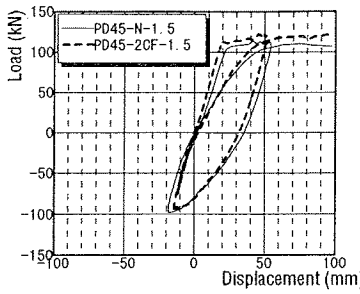

Fig. 14 Comparison of Lateral load - displacement response curves (acceleration equivalent to 450 gal)

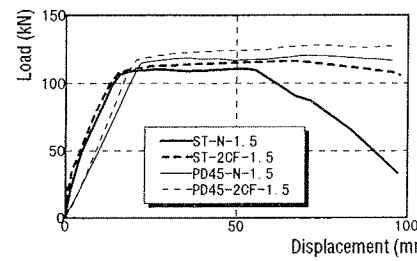

Fig. 15 Comparison of envelopes of lateral load- displacement curves

Figure 15 compares the positive-side envelopes shown in Figure 14 with the positive-side envelopes of the load-displacement curves obtained with specimens ST-N-1.5 and ST-2CF-1.5 that were used in the ST load test. Because of the influence of loading speed [9], the maximum lateral load obtained in the PD experiment is about 10% larger than that obtained in the ST experiment. In addition, the loads in the PD experiment are applied under the drift of response displacement, the envelopes for ST-N-1.5 and PD 45-N-1.5 (both without CFS) markedly differ in shape. The implication of this is that load-displacement curves which are obtained experimentally vary according to the loading speed and loading method, and that when there is fear of a wide variance in lateral load due to the buckling of longitudinal bars or the shear fracturing of concrete, the loading method has an especially strong effect.

4.2 Response calculation

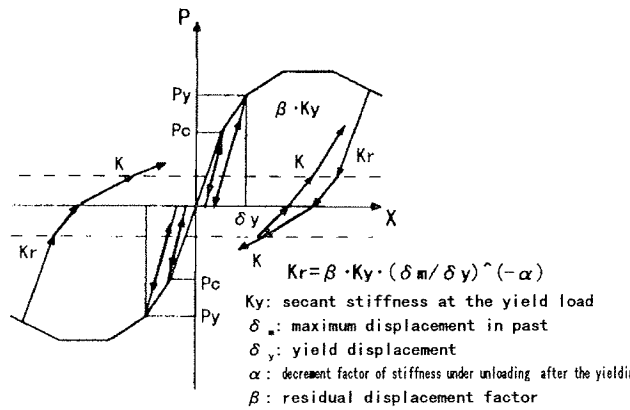

Fig. 16 Model of hysteresis loop

Figure 16 shows the analytical hysteresis loop model used in the response analysis. This model was proposed on the basis of the ordinary "stiffness degradation model" in which the unloading stiffness, after the yielding, was decreased according to the increment of the plastic ratio of the member. The features of the proposed model are that the skeleton of the

envelope curve can be expressed by many straight lines and that the stiffness under unloading can be divided into two parts, such as high loading stage and low loading stage. Also, since it is possible in this model to change the decrement ratio of the stiffness according to the number of the loading cycles, this model can express degradation due to shear failure. The stiffness under reloading is the secant modulus toward the past maximum displacement before the yielding. After yielding the stiffness is obtained by multiplying secant modulus with the decrement factor of stiffness under reloading. All factors used in this model were determined based on static test results. It should be noted, however, that the change in stiffness due to the buckling of the longitudinal bars was excluded from consideration.

Figure 17 (a) and (b) compare the differences between the measured and calculated values of the response displacement of PD 45-N-1.5 and PD 45-2CF-1.5, respectively, obtained through an experiment using an input wave equivalent to 0.2g.

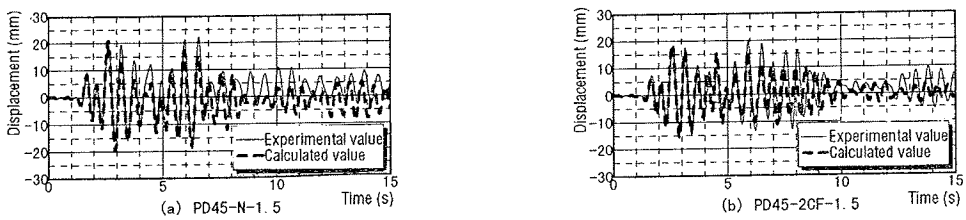

Fig. 17 Displacement response curves (load equivalent to 0.2 g)

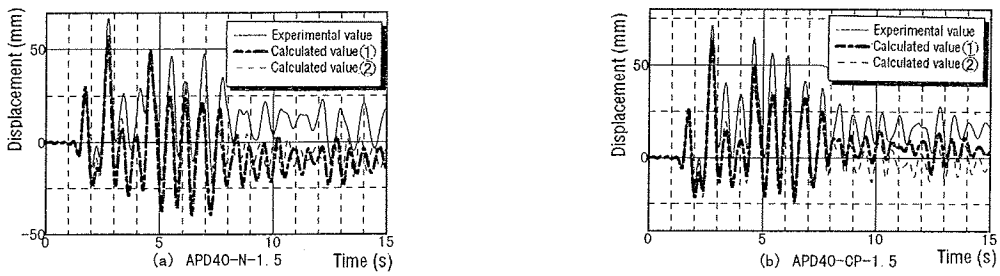

Fig. 18 Displacement response curves
(load equivalent to 400 gal--first load application)

Figure 18 (a) and (b) compare the differences between the measured and calculated values of the response displacement of APD 40-N-1.5 and APD 40-CP-1.5, respectively, obtained through the first application of an acceleration equivalent to 400gal. In the figure, calculated values ② were obtained from a model with 9.8 kN larger than the resistance against yield load in the specimen taking the speed of load application into consideration. As shown in the figure, calculated values ① and measured values ② show fairly good congruence. Thus, it was confirmed that even when the proof stress varies by about 10%, the response displacement during an earthquake remains practically unaffected.

In the experiment using an input wave equivalent to 0.2g, the longitudinal bars did not buckle, hence the experimental values show

good congruence with the calculated values. In the experiment using an acceleration equivalent to 400gal in which the longitudinal bars buckled and the resistance against lateral load declined, the response drifted after the buckling. Though the calculated values do not reflect the drift, they show good congruence with the experimental values in terms of response period and curve shape. In order to measure the response displacement behavior during an earthquake with more accuracy, it is considered effective to make a model of response displacement behavior based on the results of the PD load test.

4.3 Dynamic video images

By playing the recorded video tape at standard speed, it was possible to see the behavior of specimens under seismic load on a real-time basis. The dynamic video images revealed the instantaneous opening and closing of flexural and shear cracks, the buckling of longitudinal bars and the resulting exfoliation of concrete, the drift of response displacement to the positive or negative side due to damage, etc. In particular, in specimens reinforced with CFS, a phenomenon in which the CFS at the bottom of the column bulges across the column width and then returns to normal was observed. From the dynamic images, it was confirmed that unlike the steel jacket type reinforcement, CFS shows an elastic behavior without being subjected to local plastic deformation.

5. CFS Strain and Constraining Effect

5.1 Strain in loading direction

Figure 19 shows the load-strain curves of hoop bar and CFS in the loading direction in the area from the top end of the footing to 1*H*, obtained in the ST load test. The strain of the hoop bar of ST-N-1.5 without CFS reinforcement was about 400 μ at maximum lateral load. Thereafter, as the resistance against lateral load declined due to the buckling of longitudinal bars and the damage to the concrete, the strain increased sharply to a maximum of about 1,800 μ which was close to the yield strain. In the case of ST-2CF-1.5 with CFS reinforcement, the strain of hoop bar was not more than about 550 μ because the specimen was almost free from shear damage. The envelopes for CFS and hoop bar are similar in size and shape, and the strains of CFS and hoop bar were nearly the same at each stage of loading.

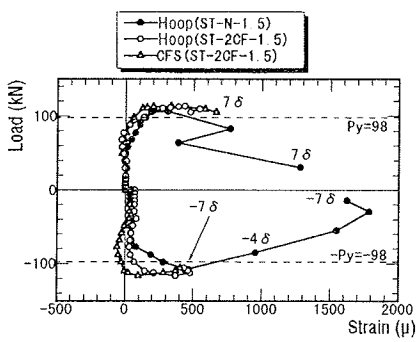

Fig. 19 Load-strain curves (aspect ratio: 1.5)

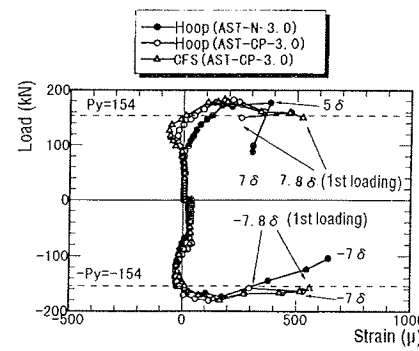

Fig. 20 Load-strain curves (aspect ratio:3.0)

Figure 20 compares the load-strain curves for specimens having an aspect ratio of 3.0. In terms of general behavior, they are very similar to specimens having an aspect ratio of 1.5. It should be noted, however, that the strain of the hoop bar of AST-N-3.0 without CFS reinforcement was not more than about 650 μ because the damage characteristics at the bottom of the column was different from that of the specimen having an aspect ratio of 1.5.

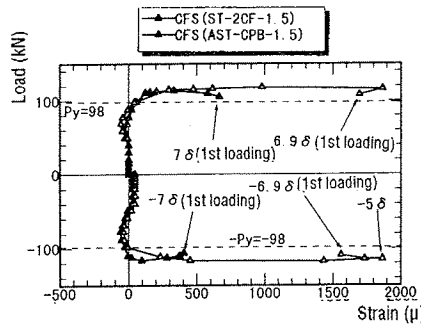

Fig. 21 Relationship between lateral load and CFS strain (ST-2CF-1.5, AST-CPB-1.5)

Figure 21 compares the CFS strains of ST-2CF-1.5 and AST-CPB-1.5 in which the bonding area of CFS was reduced to one-fourth. The strain of AST-CPB-1.5 increased sharply from around 3 δy and reached a maximum of about 2,000 μ, nearly fourfold that of ST-2CF-1.5. The reason for this is considered to be the smaller bonding area of CFS invited cracks in the shear plane.

5.2 Strain in plane perpendicular to loading direction

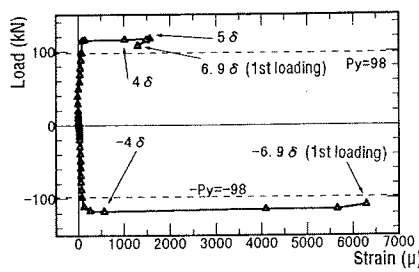

(a) CFS (south side--horizontal direction)

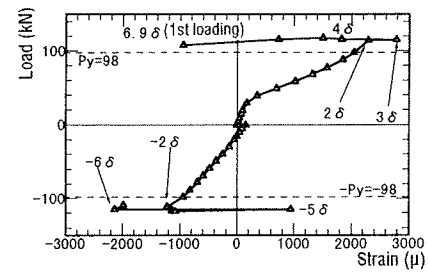

(b) CFS (south side--vertical direction)

Fig. 22 Load-CFS strain relationship (AST-CPB-1.5)

Figure 22 (a) and (b) show the CFS load-strain relationships in AST-CPB-1.5 measured by the gage at which the center of the negative side (south side) at the height of $H/2$ from the top end of the footing. With the buckling of longitudinal bars, tensile strain in the horizontal direction increased sharply to a maximum of about 6,000 μ. Ultimately the CFS fractured at column corners. From the yield strain, it is considered that the corners were subjected to a complex force, including flexure and shear, arising from the bulging of the CFS. Strain in the

vertical direction showed a complicated behavior due to the buckling of longitudinal bars, the exfoliation of concrete, etc. In terms of absolute value, it was not so large--a maximum of 2,800 μ for tensile strain and a maximum of about 2,000 μ for compressive strain.

The load-strain relationship of AST-CP-3.0 having an aspect ratio of 3.0 was similar to that of the specimens having an aspect ratio of 1.5. The maximum measured strain was 5,000 μ in the horizontal direction, 2,800 μ for tensile strain, and about 1,200 μ for compressive strain in the longitudinal direction. The CFS of this specimen did not fracture.

Figure 23 shows the response of strain in the longitudinal direction of CFS of PD 40-CP-3.0 measured in the PD load test at the center of the positive side (north side) at a height of 0.3*H*. In this specimen, only the longitudinal bars on the negative side (south side) buckled, causing the displacement response to drift to the positive side. Unlike the case in the ST load test, the measured compressive strain peaked as high as about 8,500 μ. After the drift of displacement, it was fluctuating between 2,000 μ and 4,000 μ. When PD 45-2CF-1.5 (aspect ratio: 1.5) was subjected to a load equivalent to 450 gal, the specimen showed deformation marked only to the positive side. As a result, the longitudinal bars did not buckle and the CFS compressive strain on the positive side peaked as high as about 12,000 μ. Thus, the maximum compressive strain of CFS is largely dependent on the load history, failure mode, and measuring point.

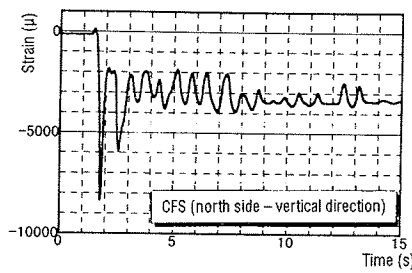

Fig. 23 Longitudinal strain response of CFS (PD 40-CP-3.0, load equivalent to 400 gal)

Judging from the measured strain values, it is the time when the covering concrete begins to bulge due to the buckling of longitudinal bars, etc. that the confinement effect of CFS makes itself felt. Even when the concrete inside the CFS broke into pieces, the CFS was displaying its confinement effect. It was confirmed that exfoliation of CFS from the concrete does not occur at the bonded surface but that a thin layer of concrete surface exfoliates from the pier itself.

6. Conclusions

The results of the present study are summarized below.

(1) It was confirmed that reinforcement with CFS is effective to improve the seismic performance and ductility of the reinforced concrete piers under consideration (existing piers).
(2) By using an area ratio of 0.1% for CFS reinforcement, the ductility ratio of the existing piers could be improved to 7 or greater.

(3) It was found that from the viewpoint of improving ductility, the area of reinforcement from the top end of the footing to 1*H* (*H*: height of cross section) is important.
(4) Reinforcement with CFS also improves the deformation capacity of a wall-type bridge pier having an aspect ratio of 3.0. However, the effect of CFS was less conspicuous than in a bridge pier having an aspect ratio of 1.5.
(5) AST-CPB-1.5 in which the area of bonding between CFS in the loop direction and concrete was 1/4 of that of ST-2CF-1.5 showed almost the same load-bearing behavior as ST-2CF-1.5. Thus, the effect of bonding on ductility was considered small. It should be noted, however, that in the case of ST-CPB-1.5, the CFS in the hoop direction ultimately fractured.
(6) It was confirmed that the existing piers had sufficient seismic performance against a seismic wave equivalent to 0.2 g, which is the assumed value in seismic design. They were free from both major damage and a marked decline in resistance against lateral load.
(7) It was clarified that when reinforced with CFS, with an area ratio of 0.1%, the existing piers would show a sound load-bearing behavior, without suffering a marked decline in resistance against lateral load, during a seismic wave equivalent to 400 gal which is about two times the seismic wave assumed in seismic design. Even during the second application of a load equivalent to 400 gal, assuming an after tremor, no marked decline in resistance against lateral load was observed. Thus, reinforcement with CFS was also found effective in securing bridge pier safety during an after tremor.
(8) Reinforcement with CFS ultimately reduced the number of areas of damage in members, as well as the range of damage.
(9) The displacement response of members measured by a load test varies according to the method of load application. In particular, the method of load application significantly influences members whose resistance fluctuates greatly due to the buckling or shear fracture of longitudinal bars.
(10) The results of a response calculation confirmed that an increase in lateral load, not exceeding about 10%, caused by a strain velocity would not influence the displacement response behavior during an earthquake.
(11) From dynamic video images, the elastic behavior of CFS--bulging and restoring--caused by the buckling of longitudinal bars could be seen clearly. Any local plastic deformation of CFS was not observed.
(12) It was confirmed that CFS in the hoop direction fractures at the column corners first.
(13) The maximum compressive strains in CFS measured with various specimens range widely from 1,000 μ to 12,000 μ. It was found that the maximum compressive strain shows marked variation according to load hysteresis, failure mode, and measuring point.

[Acknowledgments]

In carrying out the present study, we obtained the cooperation of Mr. Yutaka Morishita, technical official of civil engineering, Mr. Wataru Harayama, and Mr. Masahiro Tsuji, graduate students, of Yokohama National University. Much help was extended to us from Mr. Shozo Ohtani and Mr. Seiji Ohkawa, both from Japan Highway Public Corporation. We wish to express our heartfelt thanks to all persons concerned, including Mr. Naoki Kuwata (Mabuchi Construction Co.), Mr. Akira Kobayashi (Tonen), and Mr. Hiroshi Harashima (Taisei Service Co.), for their

generous cooperation.

References

[1] Uji, K., "Improvement of Shear Capacity of Existing Reinforced Concrete Members with Sheet Type Carbon Fiber Reinforcement" (in Japanese), Concrete Research and Technology, Vol. 3, No. 2, pp.37-47, July 1992
[2] Okajima, T., Katsumata, H., Ohno, R. and Odajima, T., "Seismic Retrofit of Existing Reinforced Concrete Bridge Piers Using Carbon Fibers: Phase 2 Loading Tests" (in Japanese), Proceedings of the 45th annual lecture meeting of the Japan Society of Civil Engineers, Part Five, pp.824-825, Sep. 1990
[3] Fujiwara, H., Higashida, N., Ohono, R., and Odajima, T., "Seismic Retrofit Effects by Carbon Fibers for Reinforced Concrete Bridge Piers: Phase 1 Loading Test" (in Japanese), Proceedings of the 46th annual lecture meeting of the Japan Society of Civil Engineers, Part Five, pp.770-771, Sep. 1991
[4] Yamaguchi, T., Takemura, H.,Yanai, S., and Ikeda, S., "Seismic Properties and Dynamic Response Behavior of Reinforced Concrete Columns" (in Japanese), Proceedings of Japan Concrete Institute, Vol. 16, No. 2, pp.1265-1270, 1994
[5] Sakai, S., Yusa, K., Yanagi, S., Yoshida, M., "Reparments and Reinforcement Method of Two Span Continuous Box Girder Bridge", Japan Prestressed Concrete Engineering Association, Vol. 37, No.6, pp.33-41, November 1995
[6] Yanai, S., Yamaguchi, T., and Ikeda, S., "Study on Dynamic Visualization for Seismic Response of 2-story Reinforced Concrete Rigid Frames"(in Japanese), Proceedings of Japan concrete Institute, Vol. 17, No. 2, pp.481-486, 1995
[7] Uji, K., "Study on the Strengthening and Enhancement of Durability by using Sheet Type Carbon Fiber Reinforcement", doctoral thesis of Yokohama National University, March 1993
[8] Ikeda, S., Yamaguchi, T., and Uzawa, T., "Response of Reinforced Concrete Columns Subjected to Earthquake Forces and Evaluation of Seismic Design" Concrete Research and Technology, Vol. 2, No. 1, pp.105-114, Jan. 1991
[9] Yamaguchi, T., Takemura, Y., and Ikeda, S., "Effect of Strain Viscous Damping on Pseudo-dynamic Test of Reinforced Concrete" Concrete Research and Technology, Vol. 7, No. 2, pp.143-155, July 1996.
[10] Japan Road Association, "SPECIFIATIONS FOR HIGHWAY BRIDGES, PART V :SEISMIC DESIGN,"(Japanese) Feb. 1990, (English) Oct. 1993